Modeling of Photovoltaic System with modified Incremental Conductance Algorithm for fast changes of irradiance

Saad Motahhir *, Abdelaziz El Ghzizal, Souad Sebti, Aziz Derouich
Laboratory of Production engineering, Energy and Sustainable Development, Higher School of Technology, SMBA University, Fez, Morocco
* Correspondence: saad.motahhir@usmba.ac.ma

Abstract The first objective of this work is to determine some of the performance parameters characterizing the behavior of a particular photovoltaic (PV) panels that are not normally provided in the manufacturers' specifications. These provide the basis for developing a simple model for the electrical behavior of the PV panel. Next, using this model, the effects of varying solar irradiation, temperature, series and shunt resistances and partial shading on the output of the PV panel are presented. In addition, the PV panel model is used to configure a large photovoltaic array. Next, a Boost converter for the PV panel is designed. This converter is put between the panel and the load in order to control it by means of a Maximum Power Point Tracking (MPPT) controller. The MPPT used is based on incremental conductance (INC), and it is demonstrated here that this technique does not respond accurately when solar irradiation is increased. To investigate this, a modified incremental conductance technique is presented in this paper. It is shown that this system does respond accurately and reduces the steady-state oscillations when solar irradiation is increased. Finally, simulations of the conventional and modified algorithm are compared, and the results show that the modified algorithm provides an accurate response to a sudden increase in solar irradiation.

Keywords Boost; Modified Incremental Conductance; Photovoltaic panel; sudden increasing of solar irradiation.

NOMENCLATURES

- a: diode's ideality factor
- I: output current of the panel [A]
- Is: diode saturation current [A]
- Iph: panel photocurrent [A]
- G: solar irradiation [W/m²]
- K: Boltzmann constant [J.K^{-1}]
- q: electron charge [C]
- R: the load [Ω]
- Req: the resistance seen by the panel [Ω]
- Rs: series resistance [Ω]
- Rsh: shunt resistance [Ω]
- T: junction temperature [K]
- V: output voltage of the panel [V]
- Vo: output voltage of the Boost converter [V]
- Io: output current of the Boost converter [A]
- F: switching frequency [Hz]
- ΔV: input voltage ripple of the Boost converter [V]
- ΔVo: output voltage ripple of the Boost converter [V]
- ΔI_L: inductor current ripple [A]

GREEK LETTERS

- α: duty cycle

ABBREVIATIONS

- CCM: Continuous Conduction Mode
- FSCC: Fractional Short-Circuit Current
- FOCV: Fractional Open-Circuit Voltage
- INC: Incremental Conductance
- MPP: Maximum Power Point
- MPPT: Maximum Power Point Tracking
- P & O: Perturb and Observe
- PV: Photovoltaic
- STC: Standard Test Conditions

1 Introduction

The energy generated by the PV systems depends on various parameters, either environmental as temperature and irradiance or internal parameters of the PV panel, namely, the series and shunt resistors [1], [2]. Thus, the load imposes its own characteristic on the output power [3]. Therefore, in order to predict and analyze the effect of these parameters on the PV power, the model of the PV panel should be previously studied and achieved, and this model should be in accordance with the real comportment of the PV panel. Therefore, different models were proposed in the literature, in [27] a single diode model is used, in [4] a two diodes model is proposed to illustrate the influence of the recombination of carriers, and in [5] a model of three diodes is used to present the effects which are neglected by the two diodes model. However, the single-diode model is the most adopted due to its good simplicity and accuracy [15]. Moreover, manufacturers of PV panels offer only some characteristics. However, other characteristics required to model PV panel are lacked in the datasheet, as the photocurrent, the diode saturation current, the series and shunt resistors, and the ideality factor [6]. Hence, in [15]-[17] researchers have proposed different methods to extract the lacked characteristics based on the datasheet values, but these methods require an implementation and this can increase the time spent in the development of a PV application. Therefore, this paper aims firstly to extract parameters lacked in the manufacturers' datasheet by using a simple tool provided by MathWorks [28] and then model the PV panel. The single diode model is used in this work because it gives a high compromise between accuracy and simplicity [11] and several researchers have used it in their works [12], [13]. In addition, this work shows the effect of parameters that may change the performance of the PV panel. Then, this model will be a platform to design a PV array.

On the other side, the maximization of the PV power always remains a major challenge. Researchers have proposed different MPPT algorithms to maximize PV power, namely FSCC, FOCV, Fuzzy Logic, Neural Network, P&O, and INC [7], [8]. FSCC and FOCV are the simplest MPPT algorithms, which are based on the linearity of short-circuit current or open-circuit voltage to the maximum power point current or voltage. However, these techniques isolate the PV panel to measure the short-circuit current or open-circuit voltage. Therefore, the loss of energy is increased due to the periodic isolation of the panel [9]. On the other side, Fuzzy Logic and Neural Network obtain a consistent MPPT technique due to their ability to treat the nonlinearity of the PV Panel, but these techniques depend heavily on the PV panel characteristics [10], and the PV panel's characteristics change along with time due to the randomly fluctuating atmospheric conditions. Hence, the update of the algorithm parameters is required. On the other side, P&O and INC are mostly used. These techniques use the (P-V) characteristic of the PV panel. For P&O, steady-state oscillations occur after the MPP is found due to the perturbation made by this technique to maintain the MPP, which in turn this increases the loss of power [14]. For INC, it is founded in the fact that slope of P-V characteristic is zero at the maximum power, and theoretically, there is no perturbation after the MPP is found. Therefore, oscillations are minimized. However, on the implementation, the zero value is hardly found on the slope of the P-V characteristic due to the truncation error in digital processing. Thus the INC technique can make an inaccurate response when the irradiation is suddenly increased [25]. Therefore, this work aims also to propose and implement a modified INC algorithm, which can overcome the wrong response made by the conventional INC algorithm when the irradiance is suddenly increased. Therefore, this work proposes a new technique to detect the increase in solar irradiation. The variation of voltage (ΔV) and current (ΔI) are used to identify the increase in irradiation instead of the slope ($\Delta P/\Delta V$) of the P-V characteristic. The modified algorithm detects the increase of irradiance and makes a correct decision. Moreover, a mini error is accepted to admit that the slope is near to zero and minimize the steady-state oscillations.

This paper is structured as follows. Following the introduction, section two presents the modeling of PV panel and array and presents the impact of different environmental and internal parameters. Section three presents the design of the Boost converter, the conventional algorithm, and the proposed algorithm.

2 Modeling of PV Panel and Array

2.1 Model of PV Panel

As shown in Fig. 1, the single diode model of PV panel can be presented by a photocurrent source and a diode connected with series and shunt resistances. The mathematical model of the PV panel can be presented by the following equations [14]:

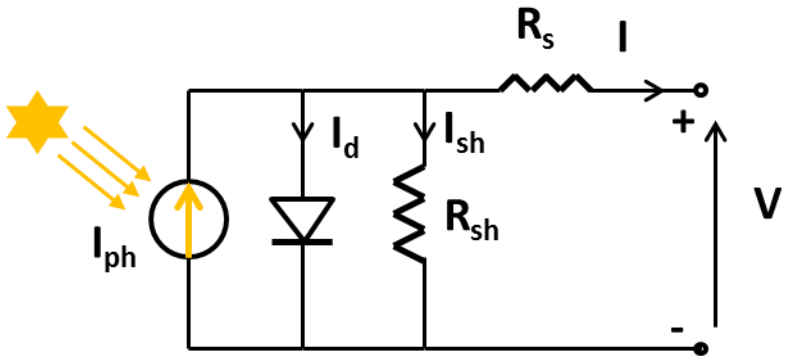

Fig. 1 PV panel equivalent circuit

$$I = I_{ph} - I_S\left(\exp\frac{q(V + R_s I)}{aKTN_s} - 1\right) - \frac{(V + IR_s)}{R_{sh}} \quad (1)$$

$$I_{ph} = (I_{SC} + K_i(T - 298.15))\frac{G}{1000} \quad (2)$$

$$I_S = \frac{I_{SC} + K_i(T - 298.15)}{\exp\left(\frac{q(V_{OC} + K_V(T - 298.15))}{aKTN_S}\right) - 1} \quad (3)$$

Hence, the physical behaviour of the PV panel depends on the shunt and series resistances, solar irradiation and temperature. Therefore, in this work, the impact of these parameters on the output of the PV panel is investigated.

The panel used in this work is MSX-60 panel, and as presented in table I, the datasheet of PV panel provides only some characteristics of PV panel. Thus, other characteristics required to model PV panel are lacked in the datasheet, as the photocurrent, the diode saturation current, the series and shunt resistors, and the ideality factor. Hence, researchers have proposed different methods to extract the lacked characteristics based on the datasheet [15]-[17]. But these methods require an implementation and this can increase the time spent in the development of a PV system. Therefore, this work aims firstly to extract these parameters by using a simple tool provided by MathWorks which is "PV array", the latter is provided in Simulink 2015 or later [28]. Hence, as shown in Fig. 2, we have only to set the datasheet values and automatically it will generate the lacked parameters.

Table I Characteristics of MSX-60 PV panel at STC

PV panel parameters	Values
Maximum power, Pmax	60 W
Maximum power voltage, Vmp	17.1 V
Maximum power current, Imp	3.5 A

Short-circuit current, Isc	3.8 A
Open-circuit voltage, Vco	21.1 V
Voltage/temp. coefficient, Kv	-0.38 %/°C
Current/temp. coefficient, Ki	0.065 %/°C
The number of cells, Ns	36

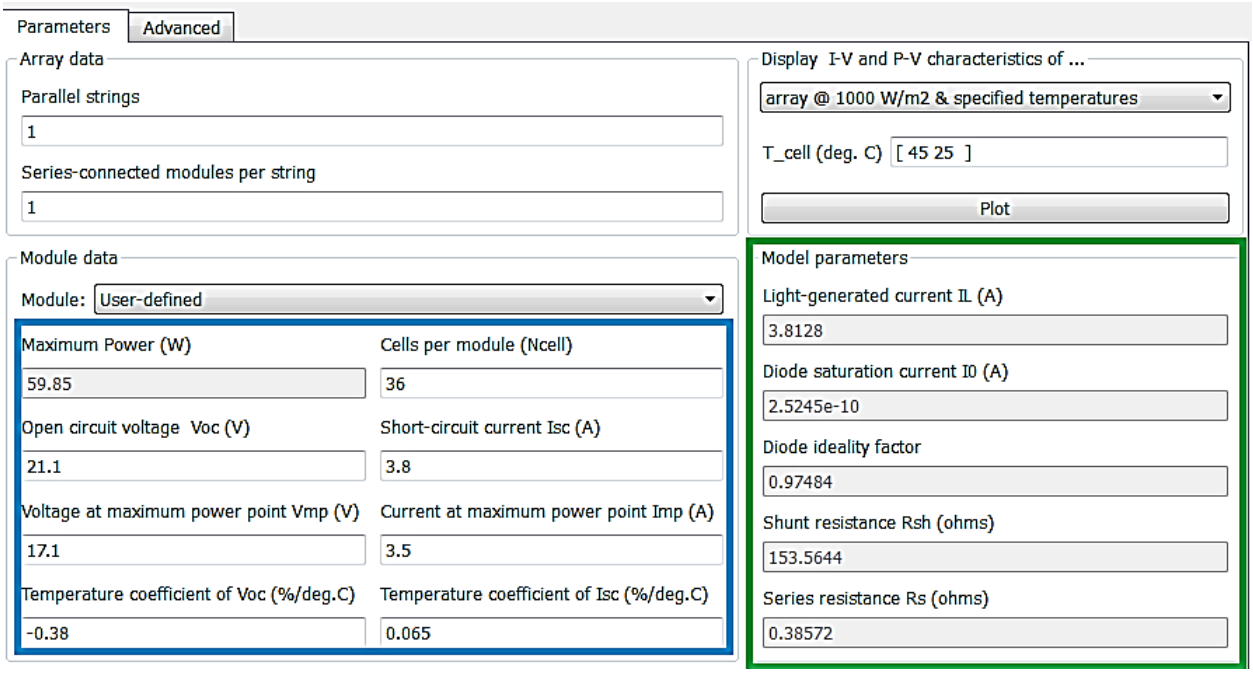

Fig. 2 PV Array tool

Equations (1), (2) and (3) are modeled using PSIM (Software for Power Electronics Simulation), and Fig. 3 presents the PSIM model.

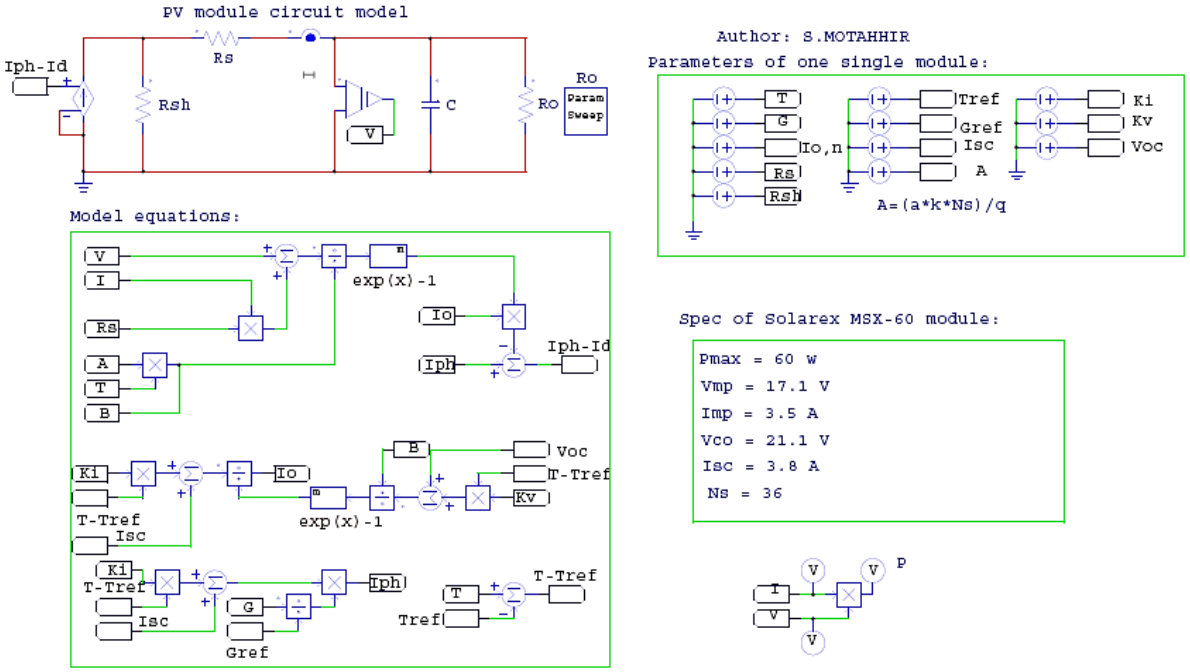

Fig. 3 PV panel PSIM model

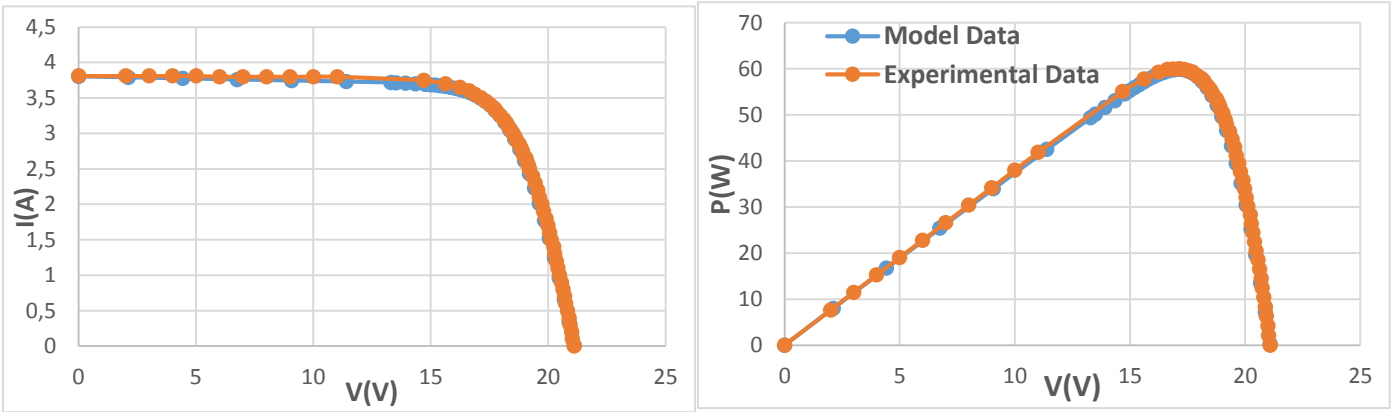

Fig. 4 I-V and P-V characteristics of model and experimental data

Fig. 4 shows the I-V and P-V curves of experimental and PSIM model under STC. The experimental data P (V) and I (V) are got from the manufactured datasheet [26]. And as presented, the model data are in accordance with the experimental data both in the current and power curves.

2.2 Effect of solar irradiation variation

The Fig.3 contains the model of the three equations: one of these equations computes the photocurrent based on temperature and irradiance (equation (2)). The model of this equation is presented in Fig.5, and Fig. 6 presents I-V and P-V curves for different values of solar irradiation.

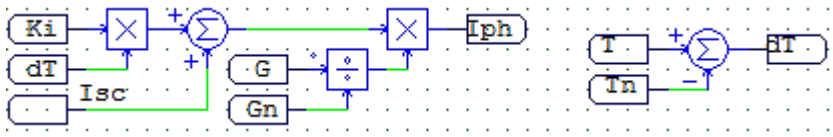

Fig. 5 Model of the equation (2)

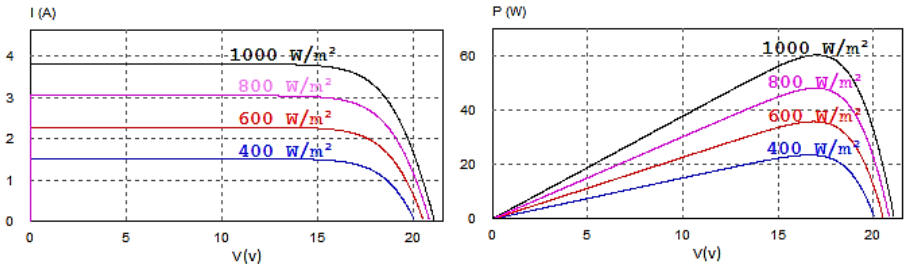

Fig. 6 I-V and P-V curves for different values of irradiance

As presented in Fig. 6, the PV panel current depends heavily on solar irradiation. However, the voltage increases just by 1 V once the irradiance is increased from 400 W/m² to 1000 W/m². Therefore, the irradiance change affects heavily the PV panel current.

2.3 Effect of the temperature variation

The Fig. 3 contains also the modeling of the equation (3), which computes the diode saturation current based on the temperature. The model of this equation is shown in Fig. 7, and Fig. 8 shows the I-V and P-V curves for different values of temperature.

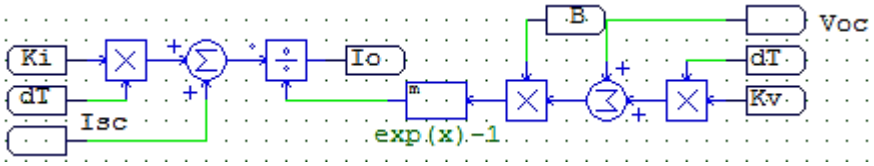

Fig. 7 Model of equation (3)

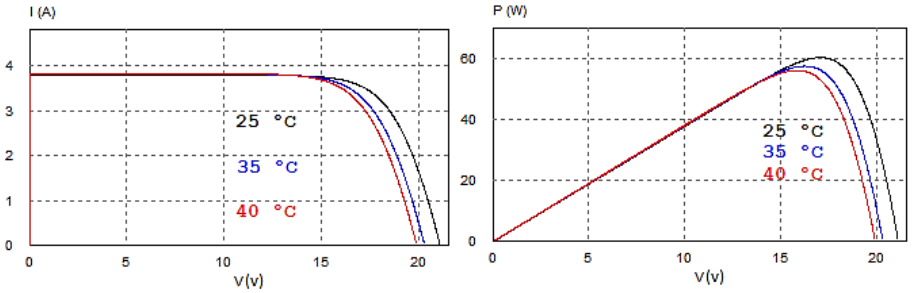

Fig. 8 I-V and P-V curves for different values of temperature

Generally, as shown in Fig. 8, for a fixed solar irradiation and when the temperature increases, the open circuit voltage decreases and the short-circuit current increases with a little value. Therefore, the temperature change affects strongly the PV panel voltage.

2.4 Effect of series resistor variation

The series resistor value is very small and it may be neglected in some cases. Nevertheless, to make the appropriate model for any PV panel, it is recommended to make a variation of this resistor and show its effect on the PV panel output. As shown in Fig. 9, the change of the series resistor results on the deviation of the MPP.

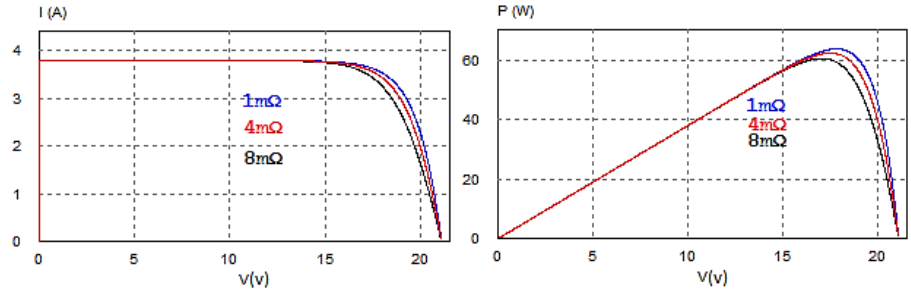

Fig. 9 I-V and P-V curves for different values of R_s

The simulation was made for three values of series resistance (1mΩ, 4mΩ, and 8mΩ). Moreover, as shown in Fig. 9, the upper values of series resistance decrease the output power. In addition, the fill factor presented by the equation (4) decreases as series resistance increases [18].

$$FF = \frac{P_{max}}{V_{OC} I_{SC}} \qquad (4)$$

2.5 Effect of shunt resistor variation

As presented in Fig. 10, The R_{sh} should be quite large for a good fill factor. In fact, when R_{sh} is small, the current collapses more strongly, then the loss of power is high and the fill factor is low. Therefore, the R_{sh} of any PV panel should be large enough for a good efficiency.

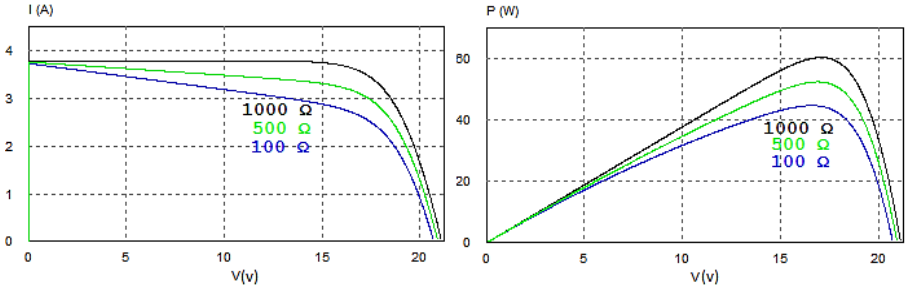

Fig. 10 I-V and P-V curves for different values of R_{sh}

2.6 Effect of shading

Partial shading also presents a major impact on PV output power. When the insolation received by a part of the PV panel (shaded cells) is less than the insolation received by another part (illuminated cells). Therefore the current generated by the illuminated cells is greater than the current produced by the shaded cells, this mismatch makes the diode of shaded cells reverse biased, which in turn the power will be lost in the shaded cells and that may cause a HOT SPOT problem which is the reason of permanent damage to the PV panel [14]. Hence in order to overcome this problem, the bypass-diodes can be connected in parallel with PV cells [14].

To simulate the effect of shading, a bypass-diode is associated with each string of the panel, and it should be mentioned that the panel used includes two strings and each string is a set of 18 cells. Thus, as shown in Fig. 11, the first string is exposed by 1000 W/m² and the second string by 700 W/m².

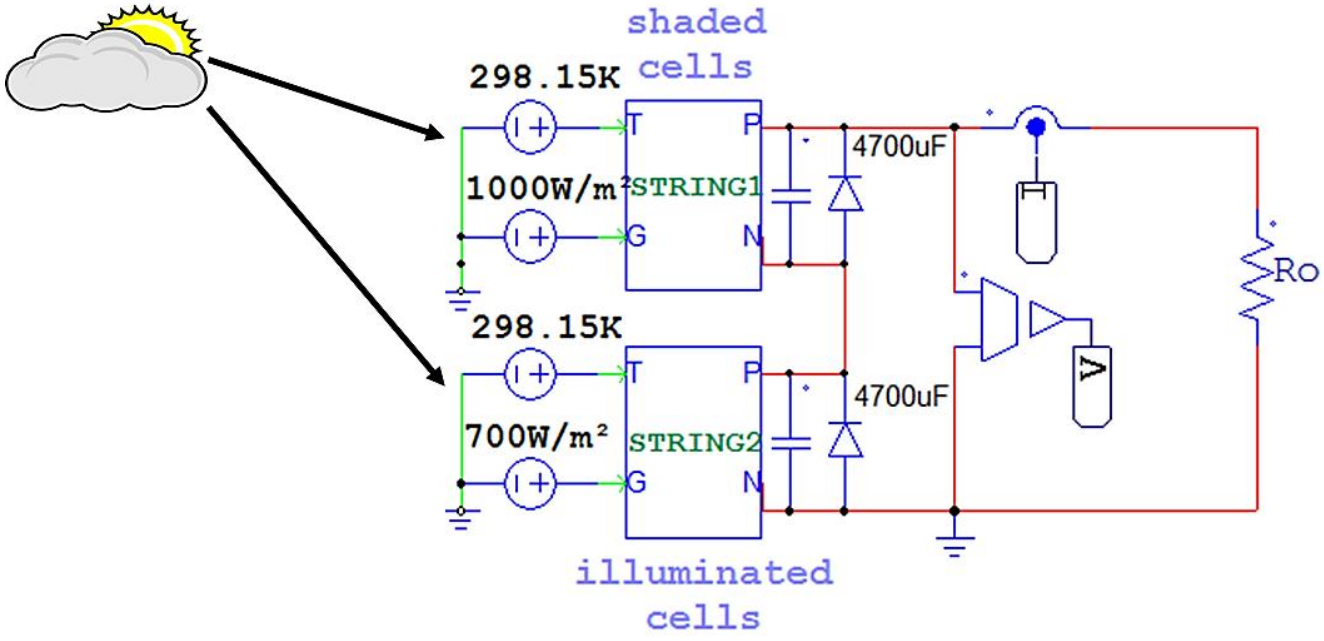

Fig. 11 PV panel under non-uniform irradiation

Under uniform irradiation, the bypass diodes have no impact because they are reverse biased. But under shading, the current flows through the bypass diode instead of the shaded string because the bypass diode is directly biased, which in turn no power will be lost in the shaded cells and only the illuminated cells generate power. Fig. 12 shows the effect of bypass diodes on the PV panel characteristics and as presented multiple peaks may occur on the P-V curve, as in this case there are two peaks, point A which is the global peak and point B which is the local peak. Therefore, conventional MPPT algorithms are unable to track the global peak which is the real MPP [14].

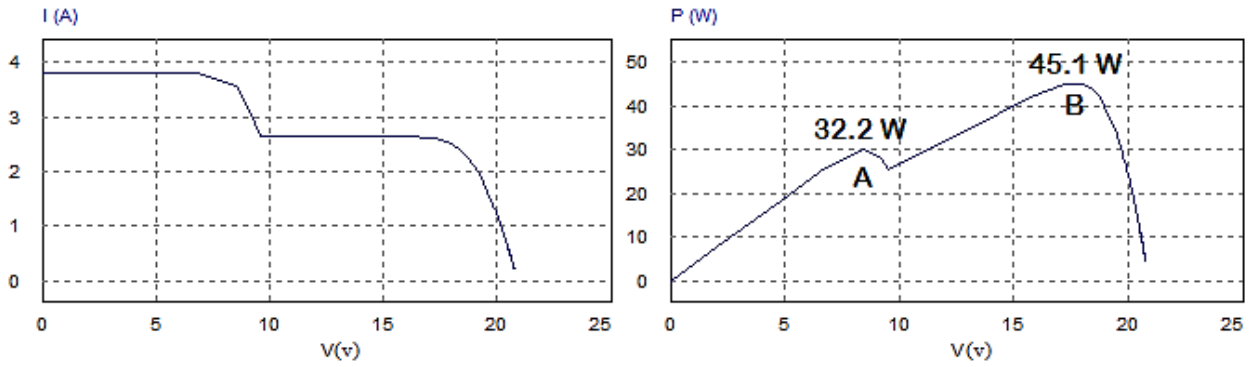

Fig. 12 I-V and P-V characteristics of the PV panel under non-uniform irradiation

2.7 Photovoltaic Array

To get benefit from the model developed, a PV array of 18 PV panels has been built in order to supply a Solar pumping station, not studied in this paper. Therefore, as shown in Fig. 13, three strings of six PV panels have been linked in parallel and each group is composed of six panels in series.

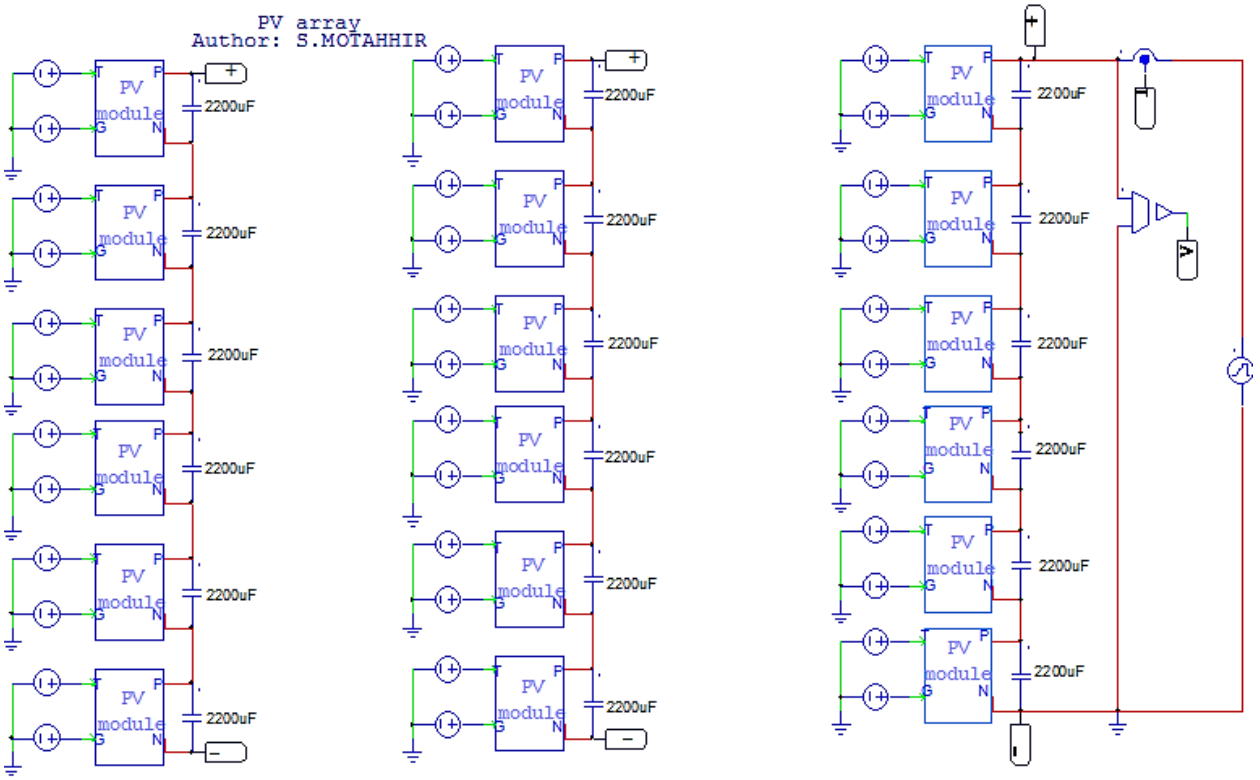

Fig. 13 PV Array model

The model of the PV array has been achieved on PSIM, and simulation result obtained is presented in Fig. 14.

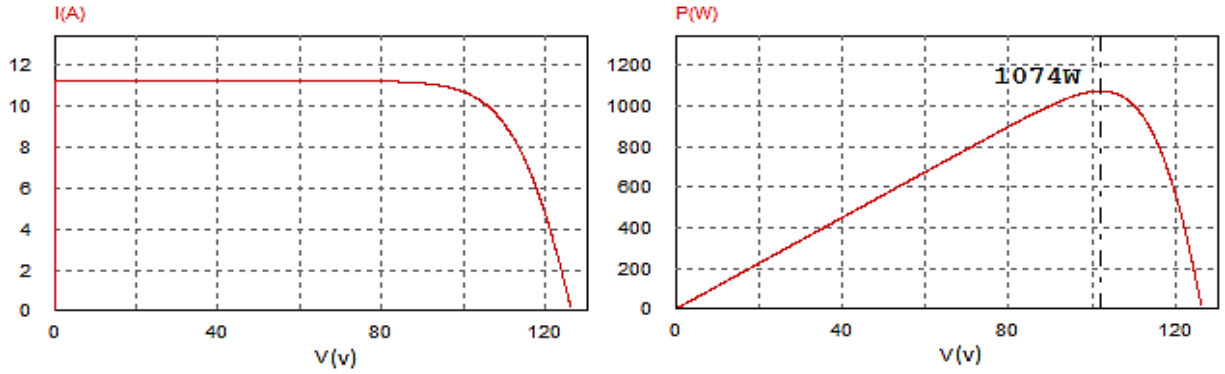

Fig. 14 I-V and P-V curves of the PV Array

As presented in Fig. 14, the panels connected in parallel increase and the current the panels connected in series increase the voltage. However, as discussed in the previous section, this connection between panels can lead to HOT-SPOT problem when the insolation received by a part of the PV array (shaded panels) less than the insolation received by another part (illuminated panels).

3 Modified INC algorithm with Boost converter

PV panel provides I-V and P-V curves presented in Fig. 15, these curves highlight one point where the power is maximum. As presented above, this point depends on solar irradiation temperature. Moreover as presented in Fig. 15, in general the load's characteristic is different from the MPP. Therefore, the Boost converter controlled by a duty cycle (α) generated by the MPPT controller is put between the panel and the load [19]. The interest of this addition is to remove the

mismatch between the panel and the load, and then the PV panel can operate at MPP.

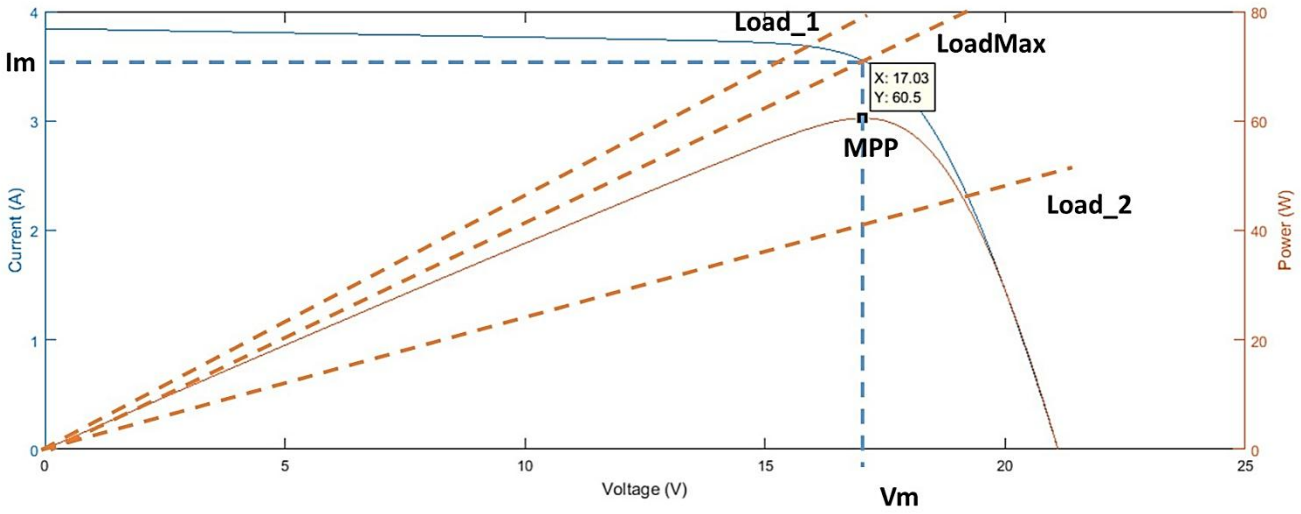

Fig. 15 The impact of load on I-V and P-V characteristics

3.1 Boost converter design

Fig. 16 presents the circuit of the boost converter, this converter is used as an adapter between the source and the load. [20].

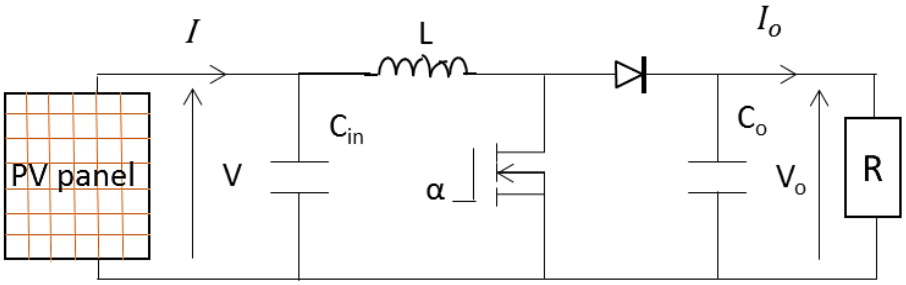

Fig. 16 Boost converter

The operation principle of this converter is described by the equations below [21]:

$$V_O = \frac{V}{(1-\alpha)} \qquad (5)$$

$$I_O = I(1-\alpha) \qquad (6)$$

By using equations (5) and (6), equation (7) is obtained, which is the relationship between the resistance seen by the PV panel (R_{eq}) and the load resistance (R). Hence, based on this equation, the MPPT controller can find the optimum α to remove the mismatch between the load and MPP. Therefore, The boost converter is required to get maximum power available from the panel.

$$R_{eq} = \frac{V}{I} = \frac{V_O(1-\alpha)^2}{I_O} = R(1-\alpha)^2 \qquad (7)$$

Selection of the inductor:

The choice of the inductor can directly influence the performance of the Boost converter. Moreover, the selection of the inductance is a trade-off between its cost, its size, and the inductor current ripple. A higher inductance value results in a minor inductance current ripple; however, that results in a higher cost and larger inductor's size, which means a larger PCB surface.

By the way, the inductance value can be given as:

During T_{ON} state:

$$V = L\frac{\Delta I_L}{T_{ON}} => L = \frac{V\alpha}{\Delta I_L F} \qquad (8)$$

Where ΔI_L can be computed as below, and r is the inductor current ripple ratio, which is optimal in the range [0.3, 0.5] [22]:

$$\Delta I_L = r \times I \qquad (9)$$

Therefore, the optimum inductor value can be computed by using equation (10):

$$L \geq \frac{V\alpha}{rIF} \qquad (10)$$

Based on Fig. 17, in order to guarantee the performance of Boost converter in the continuous conduction mode, the following equation must be verified:

$$I \geq \frac{\Delta I_L}{2} => \Delta I_L \leq 2I \qquad (11)$$

Therefore,

$$L \geq \frac{\alpha(1-\alpha)^2 R}{2F} \qquad (12)$$

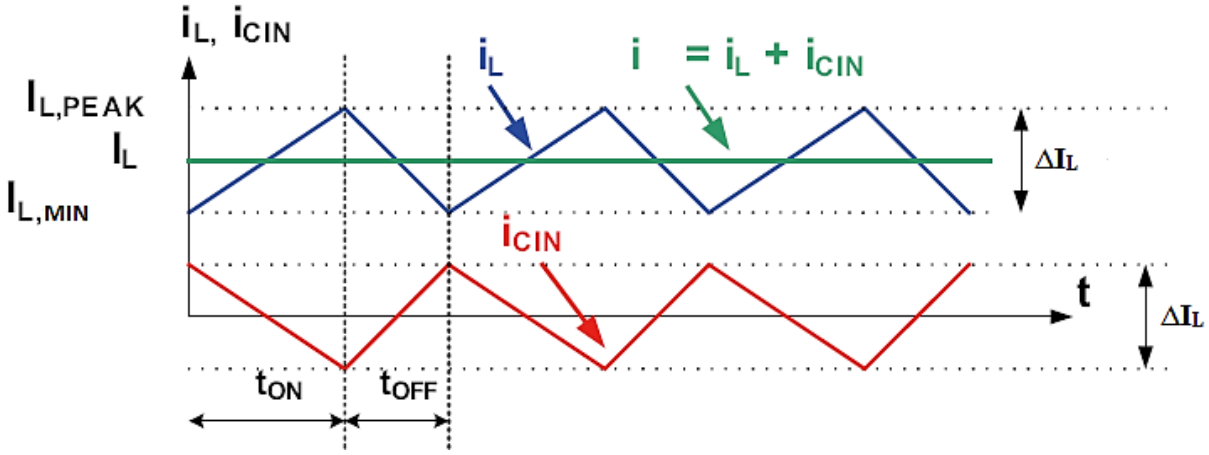

Fig. 17 Current waveforms of the input capacitor and inductor in CCM

Selection of the output capacitor:

The choice of the output capacitor is made by using output voltage ripple as follows:

During T_{ON}:

$$I_O = C_O\frac{\Delta V_O}{T_{ON}} => C_O = \frac{\alpha I_O}{\Delta V_O F} \qquad (13)$$

Therefore, the output capacitor value can be calculated as below, where the desired ΔV_o equals to 2% of output voltage [20]:

$$C_O \geq \frac{\alpha}{0.02 \times F \times R} \qquad (14)$$

Selection of the input capacitor:

An input capacitor is used to decrease the input voltage ripple and to deliver an alternative current to the inductor. The input voltage ripple matches to the charge voltage during the charge phase of the capacitor, and during this phase, I_{cin} is greater than zero, so this phase is illustrated by the blue area in Fig.18, therefore this area is used to calculate the input capacitor as follows:

$$I_{Cin} = C_{in} \frac{\Delta V}{\Delta t} => \Delta V = \frac{I_{Cin} \Delta t}{C_{in}} \qquad (15)$$

Based on Fig. 18, and by using equation (15):

$$\Delta V = \frac{\Delta I_L}{8FC_{in}} => C_{in} = \frac{\Delta I_L}{8F\Delta V} = \frac{V\alpha}{8F^2 L \Delta V} \qquad (16)$$

Therefore, the input capacitor can be calculated by equation (17), where the desired ΔV equals to 1% of input voltage [23]:

$$C_{in} \geq \frac{\alpha}{8 \times F^2 \times L \times 0.01} \qquad (17)$$

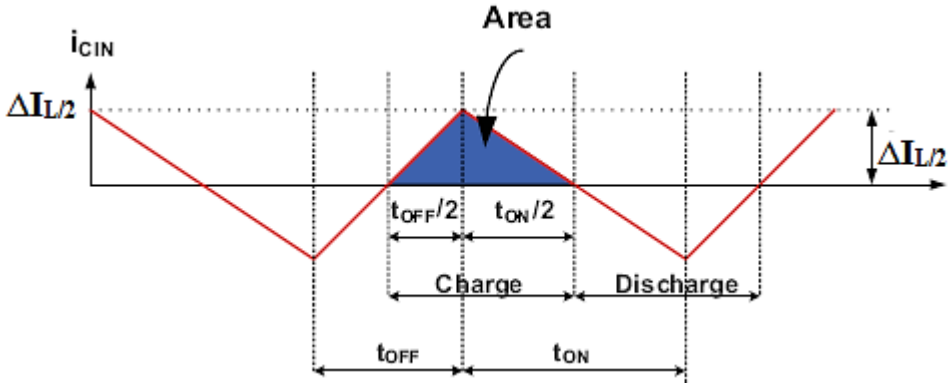

Fig. 18 Current waveforms of the input capacitor in CCM

The design of the used Boost is presented in table II.

Table II Design of the Boost converter

Parameters	Values
L	1.2 mH
C_{in}	75 µF
C_o	75 µF
F	10 kHz
R	50 Ω

α_{MPP}	0.69

3.2 Problem with the Conventional INC algorithm

A good MPPT algorithm balances between the tracking speed and steady-state performance. In accordance with these requirements, the INC algorithm can be used even if it can fail in some cases [25] and in this study, it will be modified in order to improve its performance. INC algorithm is founded in the fact that slope of P-V characteristic is zero at the MPP [24]. Therefore, this algorithm can be modeled as follows:

$$\frac{dP}{dV} = 0 \text{ at MPP} \quad (18)$$

$$\frac{dP}{dV} > 0 \text{ left to MPP} \quad (19)$$

$$\frac{dP}{dV} < 0 \text{ right to MPP} \quad (20)$$

Since:

$$\frac{dP}{dV} = \frac{d(IV)}{dV} = V\frac{dI}{dV} + I \quad (21)$$

Therefore:

$$\frac{dI}{dV} = -\frac{I}{V} \text{ at MPP} \quad (22)$$

$$\frac{dI}{dV} > -\frac{I}{V} \text{ left to MPP} \quad (23)$$

$$\frac{dI}{dV} < -\frac{I}{V} \text{ right to MPP} \quad (24)$$

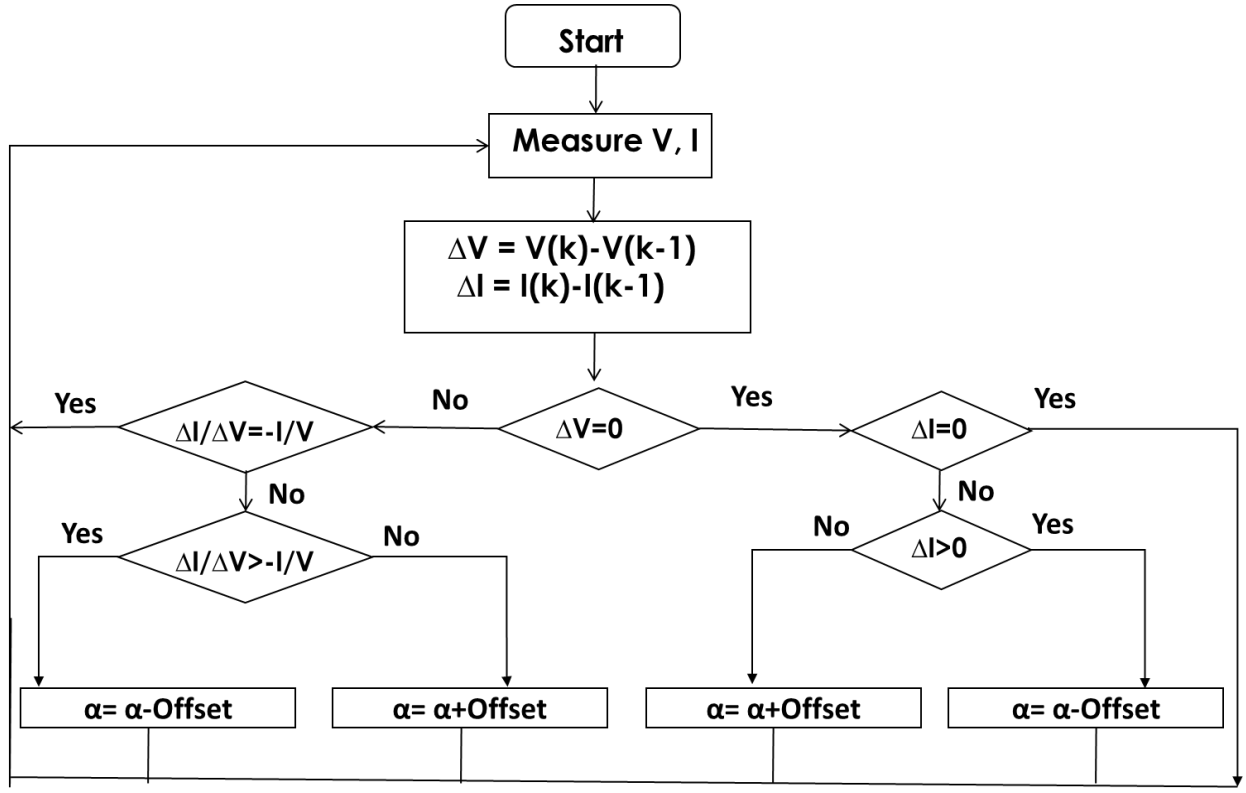

Fig. 19 Flowchart of INC algorithm

The flowchart of the INC algorithm is presented in Fig. 19 [24]. This algorithm measures the current and voltage of the panel. If equation (24) is met, the duty cycle is increased, and vice versa if equation (23) is met. Then, there is nothing to do if equation (22) is met. Therefore, theoretically, if MPP is reached, no more perturbation of α, which in turn steady-state oscillations are decreased, and that is the main advantage of INC algorithm.

However, the conventional INC algorithm fails to make a good decision when the irradiance is sudden increased [25]. As presented in Fig. 20, once the solar irradiance is at 500 W/m² and the PV system operates at load_2, the INC technique controls the PV system in order to reach the MPP (point *B*). When the irradiance is increased to 1000 W/m², Load_2 will lead the system to point *G* in I-V characteristic, which matches to point C in P-V characteristic. The INC technique calculates the slope between point *C* and point *B* which is positive. Therefore, the INC algorithm will decrease the duty cycle and consequently, the PV panel voltage will be increased. But since the MPP of 1000 W/m² is at point *A*, and the slope between point *A* and *C* is negative, then the PV panel voltage should be decreased in order to reach point *A*, instead of increase voltage and recede from point *A* as made by the conventional INC algorithm. In addition, as presented in Fig. 6, generally when the solar irradiance increases, the MPP moves to the right and consequently, the same problem will occur.

Conversely, this weakness does not happen if the solar irradiation is decreased. Because as shown in Fig. 20, the slope is positive between point *A* and *D*, and also between point *B* and *H*.

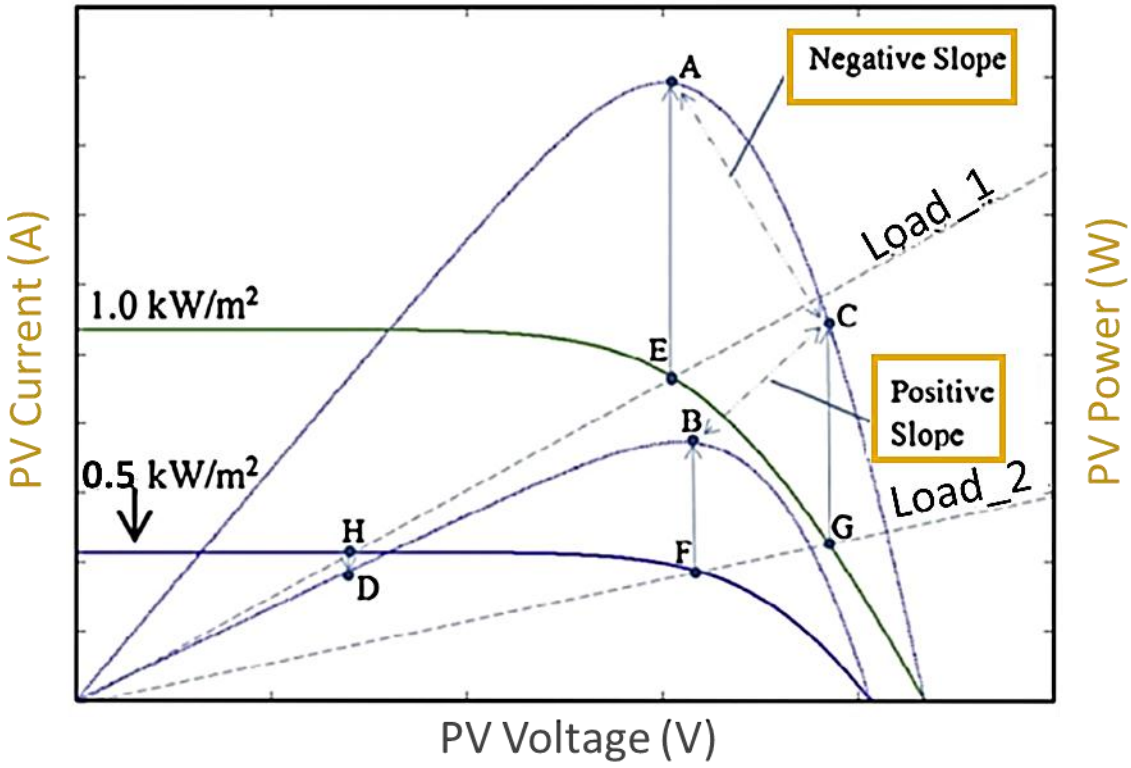

Fig. 20 P-V and I-V curves for solar irradiation 500 W/m² and 1000 W/m²

3.3 Modified INC algorithm

Based on the above analysis, it is noted that when the solar irradiance increases, both the voltage and the current are increased. Therefore, the sudden increase in solar irradiation can be detected, by checking if the MPP was reached and both the voltage and current are increased. Therefore, a permitted error is accepted (equation (25)) to stabilize our system around MPP and detect that the MPP is reached.

$$\left|\frac{dI}{dV}+\frac{I}{V}\right|<0.07 \qquad (25)$$

The proposed algorithm is presented in Fig.21. So as shown, the addition is the check if the MPP was reached by using equation (25), then set *Var* to one. After that when the equation (25) is not met and *Var* is one, the proposed technique checks if both voltage and current are increased, in this case, the duty cycle is increased instead of decreased as made by the conventional algorithm. Hence, the INC algorithm is modified to overcome the incorrect decision made by the conventional algorithm when the irradiance is increased.

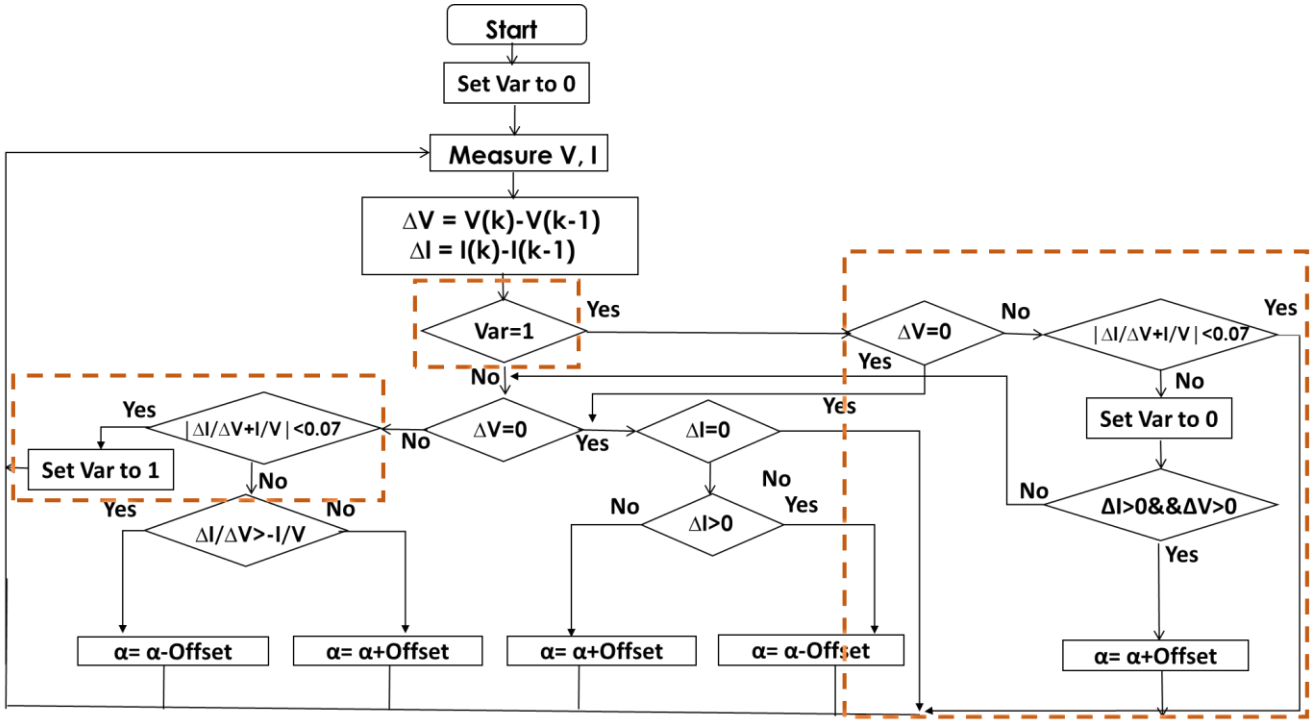

Fig. 21 Flowchart of the proposed INC algorithm

3.4 Results and discussions

The test was made for the conventional and the proposed techniques. At first, the solar irradiance is suddenly increased from 500 W/m² to 1000 W/m² at t = 0.11 s, and then it is decreased from 1000 W/m² to 500 W/m² at t = 0.23 s. Fig. 22 shows the test result of the conventional technique and Fig. 23 shows the test result of the proposed technique. Therefore, as shown in these figures, the steady-state oscillations are minimized by using the proposed and admit an error equal to 0.07. Contrary to the conventional algorithm, the power oscillates between (28.5-29.8 W), and this can generate a loss in PV energy.

In addition, as presented in Fig. 22, by using the conventional algorithm, when solar irradiation is suddenly increased, the power diverges with a value greater than 62 W and after that, the conventional INC reverses the direction and the power diverges with a value lower than 56 W and like that, the system takes a long time to converge around MPP. That is due to the wrong decision made by the conventional technique. Also even if the MPP is reached, the power oscillates between (59-61 W). On the other side, as presented in Fig. 23, the proposed technique detects the fast increase of irradiance and makes a correct decision in duty cycle. As a result, the power converges to the new MPP from the first step and it is maintained at it (60 W). In addition, it only needs 0.001 s to reach the MPP. This in turn by using the proposed INC, the power converges faster compared with the conventional algorithm which needs more time to reach the MPP.

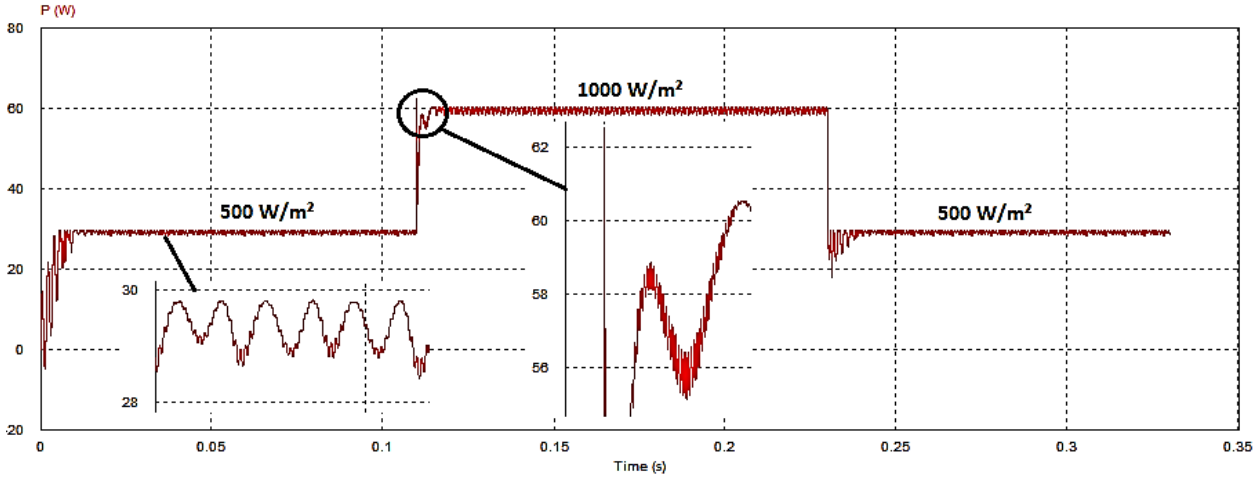

Fig. 22 Test result of the INC algorithm

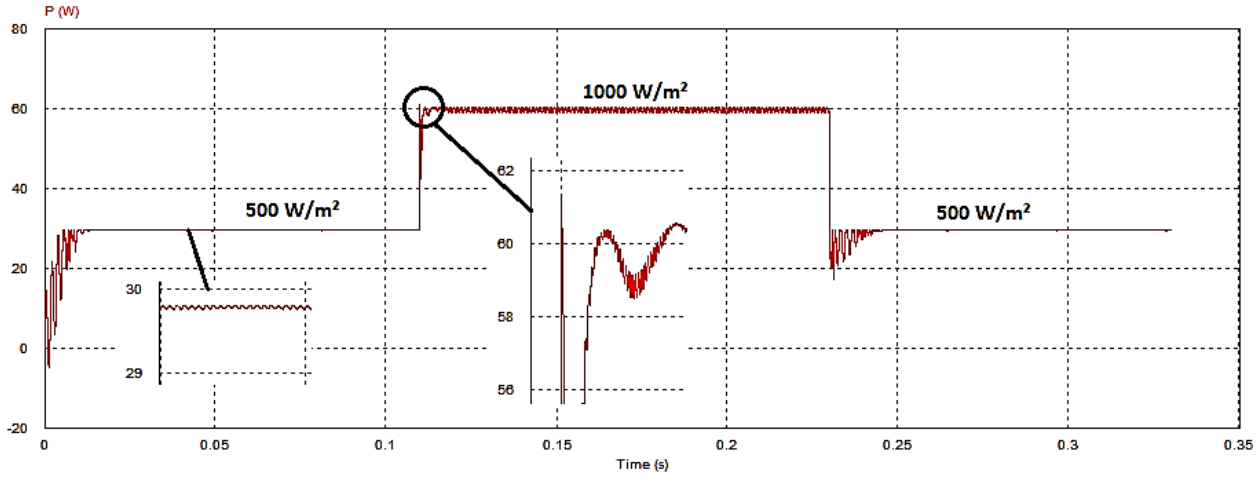

Fig. 23 Test result of the modified INC algorithm

Table III Comparison of the proposed algorithm with other improved incremental conductance algorithms proposed in scientific literature

Technique	Oscillations level	Efficiency	Response time during sudden increase in irradiation	Incorrect decision under sudden increase of irradiation
Conventional	2.5 W	96 %	Slow	Yes
[29]	1 W	96.40 %	Fast	No
[30]	1.5 W	98.5 %	Fast	Yes
[31]	1 W	97.5 %	Medium	Yes
Proposed	Neglected	98.8 %	Very fast	No

Table III summarizes a comparison of the proposed technique to other improved INC techniques proposed in the scientific literature in term of the Oscillation level, tracking efficiency, the response time during sudden increase in irradiation, and if the technique makes an incorrect decision under sudden increase of irradiation. As presented, the proposed technique shows a very fast tracking speed, a higher efficiency, and neglected oscillations around the MPP compared to other techniques. Thus only the proposed algorithm and that proposed in [29] make a correct decision

under sudden increase of irradiation, contrary to the conventional technique and those proposed in [30], [31] which make an incorrect decision.

Conclusion

In this paper, the PV panel's parameters are found using Mathworks tool, hence by using these parameters a PV panel and a PV array are modeled, and the results show that the model is in accordance with experimental data of used panel (MSX-60). In addition, a modified INC algorithm which can overcome the confusion faced by the conventional INC technique is proposed in this paper. As a result, the tests show that the modified technique detects the fast increase of irradiation and makes a correct decision, contrary to the conventional technique. Moreover, by using the modified algorithm steady-state oscillations are almost neglected. Hence, the loss of energy is minimized, which in turn the efficiency is equal to 98.8 % instead of 96 % obtained by the conventional technique.

As a perspective, the modified INC algorithm can be more improved and then implemented in an embedded hardware device.

Conflict of interest

The authors declare that they have no conflict of interest.

References

[1] Patel, H., & Agarwal, V. (2008). MATLAB-based modeling to study the effects of partial shading on PV array characteristics. IEEE transactions on energy conversion, 23(1), 302-310.

[2] Motahhir, S., Chalh, A., Ghzizal, A., Sebti, S., & Derouich, A. (2017). Modeling of Photovoltaic Panel by using Proteus. Journal of Engineering Science and Technology Review, 10 (2), 8-13.

[3] Motahhir, S., El Ghzizal, A., Sebti, S., & Derouich, A. (2015). Proposal and Implementation of a novel perturb and observe algorithm using embedded software. In 3rd International Renewable and Sustainable Energy Conference (IRSEC), (pp. 1-5). IEEE.

[4] Barth, N., Jovanovic, R., Ahzi, S., & Khaleel, M. A. (2016). PV panel single and double diode models: optimization of the parameters and temperature dependence. Solar Energy Materials and Solar Cells, 148, 87-98.

[5] Nishioka, K., Sakitani, N., Uraoka, Y., & Fuyuki, T. (2007). Analysis of multicrystalline silicon solar cells by modified 3-diode equivalent circuit model taking leakage current through periphery into consideration. Solar Energy Materials and Solar Cells, 91(13), 1222-1227.

[6] Ishaque, K., Salam, Z., Mekhilef, S., & Shamsudin, A. (2012). Parameter extraction of solar photovoltaic modules using penalty-based differential evolution. Applied Energy, 99, 297-308.

[7] Amir, A., Selvaraj, J., & Rahim, N. A. (2016). Study of the MPP tracking algorithms: Focusing the numerical method techniques. Renewable and Sustainable Energy Reviews, 62, 350-371.

[8] Gupta, A., Chauhan, Y. K., & Pachauri, R. K. (2016). A comparative investigation of maximum power point tracking methods for solar PV system. Solar Energy, 136, 236-253.

[9] Verma, D., Nema, S., Shandilya, A. M., & Dash, S. K. (2016). Maximum power point tracking (MPPT) techniques: Recapitulation in solar photovoltaic systems. Renewable and Sustainable Energy Reviews, 54, 1018-1034.

[10] Ram, J. P., Babu, T. S., & Rajasekar, N. (2017). A comprehensive review on solar PV maximum power point tracking techniques. Renewable and Sustainable Energy Reviews, 67, 826-847.

[11] Carrero, C., Amador, J., & Arnaltes, S. (2007). A single procedure for helping PV designers to select silicon PV modules and evaluate the loss resistances. Renewable Energy, 32(15), 2579-2589.

[12] Radjai, T., Rahmani, L., Mekhilef, S., & Gaubert, J. P. (2014). Implementation of a modified incremental conductance MPPT algorithm with direct control based on a fuzzy duty cycle change estimator using dSPACE. Solar Energy, 110, 325-337.

[13] Ahmed, J., & Salam, Z. (2016). A Modified P&O Maximum Power Point Tracking Method with Reduced Steady-State Oscillation and Improved Tracking Efficiency. IEEE Transactions on Sustainable Energy, 7(4), 1506-1515.

[14] Motahhir, S., El Ghzizal, A., Sebti, S., & Derouich, A. (2016). Shading effect to energy withdrawn from the photovoltaic panel and implementation of DMPPT using C language. International review of automatic control, 9(2), 88-94.

[15] Yıldıran, N., & Tacer, E. (2016). Identification of photovoltaic cell single diode discrete model parameters based on datasheet values. Solar Energy, 127, 175-183.

[16] Ishaque, K., & Salam, Z. (2011). An improved modeling method to determine the model parameters of photovoltaic (PV) modules using differential evolution (DE). Solar Energy, 85(9), 2349-2359.

[17] AlHajri, M. F., El-Naggar, K. M., AlRashidi, M. R., & Al-Othman, A. K. (2012). Optimal extraction of solar cell parameters using pattern search. Renewable Energy, 44, 238-245.

[18] Bayrak, F., Ertürk, G., & Oztop, H. F. (2017). Effects of partial shading on energy and exergy efficiencies for photovoltaic panels. Journal of Cleaner Production. 164, 58-69.

[19] Motahhir, S., El Ghzizal, A., Sebti, S., & Derouich, A. (2017). MIL and SIL and PIL tests for MPPT algorithm, Cogent Engineering, 4: 1378475.

[20] Sivakumar, S., Sathik, M. J., Manoj, P. S., & Sundararajan, G. (2016). An assessment on performance of DC–DC converters for renewable energy applications. Renewable and Sustainable Energy Reviews, 58, 1475-1485.

[21] Mohan, N., & Undeland, T. M. (2007). Power electronics: converters, applications, and design. John Wiley & Sons.

[22] Maniktala, S. (2012). Switching Power Supplies A-Z. Elsevier.

[23] Rashid, M. H. (2009). Power electronics: circuits, devices, and applications. Pearson Education India.

[24] Loukriz, A., Haddadi, M., & Messalti, S. (2016). Simulation and experimental design of a new advanced variable step size Incremental Conductance MPPT algorithm for PV systems. ISA Transactions, 62, 30-38.

[25] Tey, K. S., & Mekhilef, S. (2014). Modified incremental conductance MPPT algorithm to mitigate inaccurate responses under fast-changing solar irradiation level. Solar Energy, 101, 333-342.

[26] Solarex MSX60 and MSX64 photovoltaic panel, datasheet (1998). https://www.solarelectricsupply.com/media/custom/upload/Solarex-MSX64.pdf. Accessed 21 April 2017

[27] H. S. Rauschenbach. Solar cell array design handbook. Van Nostrand Reinhold, 1980.

[28] Mathworks (2015). PV Array. https://fr.mathworks.com/help/physmod/sps/powersys/ref/pvarray.html. Accessed 04 Mai 2017.

[29] Belkaid, A., Colak, I., & Isik, O. (2016). Photovoltaic maximum power point tracking under fast varying of solar radiation. Applied Energy, 179, 523-530.

[30] De Brito, M. A. G., Galotto, L., Sampaio, L. P., e Melo, G. D. A., & Canesin, C. A. (2013). Evaluation of the main MPPT techniques for photovoltaic applications. IEEE transactions on industrial electronics, 60(3), 1156-1167.

[31] Sekhar, P. C., & Mishra, S. (2014). Takagi–Sugeno fuzzy-based incremental conductance algorithm for maximum power point tracking of a photovoltaic generating system. IET Renewable Power Generation, 8(8), 900-914.